Extraterrestrial Photosynthesis by Chang'E-5 Lunar Soil

Yingfang Yao (yaoyingfang@nju.edu.cn)
Nanjing University https://orcid.org/0000-0003-4823-0094

Lu Wang
The Chinese University of Hong Kong (Shenzhen) https://orcid.org/0000-0002-4165-4022

Xi Zhu
School of Science and Engineering, The Chinese University of Hong Kong

Wenguang Tu
School of Science and Engineering, The Chinese University of Hong Kong

Yong Zhou
Nanjing University https://orcid.org/0000-0002-9480-2586

Rulin Liu
School of Science and Engineering, The Chinese University of Hong Kong

Bo Tao
School of physics, Nanjing University

Cheng Wang
Nanjing University

Xiwen Yu
College of Engineering and Applied Science, Nanjing University

Linfeng Gao
Nanjing University https://orcid.org/0000-0003-2717-8741

Yuan Cao
Nanjing Univeristy

Bing Wang
Nanjing University https://orcid.org/0000-0002-8735-9248

Zhaosheng Li
Nanjing University https://orcid.org/0000-0001-8114-0432

Wei Yao
China Academy of Space Technology

Mengfei Yang
China Academy of Space Technology

Zhigang Zou
Nanjing University https://orcid.org/0000-0003-2092-8335

junchuan Sun

School of Science and Engineering, The Chinese University of Hong Kong

Physical Sciences - Article

Keywords: lunar-surface solar energy conversion, electrocatalyst, photocatalyst, photothermal catalyst

Posted Date: November 5th, 2021

DOI: https://doi.org/10.21203/rs.3.rs-1045138/v1

Abstract

In light of significant effort conducted to manned deep space exploration, it is of high technological importance and scientific interest to develop the lunar life supporting system for long-term exploration and exploitation. And lunar in situ resource utilization offers great opportunity to provide the material basis of life supporting for lunar habitation and traveling. Based on the analysis of the structure and composition, the Chang'E-5 lunar soil sample was used for lunar-surface solar energy conversion, i.e. the extraterrestrial photosynthesis catalysts. By evaluating the performance of the Chang'E-5 lunar sample as photovoltaic-driven electrocatalyst, photocatalyst and photothermal catalysts, the full water splitting and CO2 conversion are able to be achieved with solar energy, water and lunar soil, with a wide range of product distribution, including O2, H2, CO, CH4 and CH3OH. Thus, we propose a potentially available extraterrestrial photosynthesis pathway on the moon, which could help us to achieve a 'zero-energy consumption' environment and life support system on the moon.

Main Text

Long-term survival on the moon shall be the first milestone towards the long march of manned deep space exploration[1]. Maximizing the utilization of *in situ* lunar resources, including extreme environmental temperature (-173-127ºC)[2,3] and strong solar irradiation[4], could help us build an extraterrestrial base on the moon for life-supporting and spacecraft launch/manufacture proposes.[5] Compared with other proposed extraterrestrial survival technologies[6-8], extraterrestrial photosynthesis (EP)[9] is expected to utilize the moon's environmental conditions for fuel and survival supply production. Such technology is able to operate with a wide temperature range, low energy consumption, and high energy conversion efficiency. And EP is mainly based on utilizing the human respired CO_2 and water from the moon[10] to produce oxygen and hydrocarbons. Achieving this objective could dramatically improve the feasibility and durability of human survival on the moon.

As one of the most abundant resources on the moon, lunar soil functioning as the EP catalysts is also highly desired as an important part of *in-situ* resource utilization (ISRU)[11,12]. Chang'E mission 5 (CE-5) sample provides us a great opportunity to study the lunar soil from the EP catalytic perspective. Therefore in this report, we first learnt the composition and structure of CE-5 lunar soil through detailed morphological observation and phase analyses. It thus helps us identify the possible catalytically active substances of the lunar soil. We then analyze the EP performance of CE-5 lunar soil from the photovoltaic-electrolytic, photocatalytic and photo-thermal catalytic aspects, and further proposed a feasible lunar EP strategy based on these EP performances. Our research thus allows us to lay a material foundation for realizing a "zero energy consumption" lunar life-support system.

The morphological characterization was carried out (TEM in Fig. 1a-c). Typically, the glassy phase, single crystal sheets, and porous materials were observed. The machine learning-based analysis is applied to analyze the CE-5 sample X-ray diffraction (XRD) data (Fig. 1d) and enables the possibility to predict the potential catalytically active components for EP. Surprisingly, the powder XRD (PXRD) pattern of the CE-5

sample (Fig. 1b, 3-85º) was distinct from the Apollo data (No. 12041, 5-55º)[13] (Fig. 1e). Comparably, the CE-5 sample was obtained as the youngest mare basalt samples, laden with Fe and Mg-based components, such as orthopyroxene, augite, pyroxene, while short of Si and Al-based components, including silica, plagioclase, and pigeonite (Extended Data Fig. 1, Extended Data Table 1, 2). Other characterization technologies were also applied to detect the elemental structures, including XPS, SEM, and TEM (Fig. 1f, Extended Data Fig. 2-6, Extended Data Table 3), supportive to iron- and magnesium-rich basalt. Therefore, a preliminary deduction could be made based on the investigation of PXRD patterns, whereas rutile (TiO_2)[14], ilmenite ($FeTiO_3$)[15], troilite (FeS)[16,17] could be treated as the photocatalytic (PC) materials, hapkeite (FeSi alloy)[18] as the photovoltaic-driven water electrolytic (PV-EC) materials, and orthopyroxene ((Mg, Fe)SiO_3), augite ((Ca, Na)(Mg, Fe, Al, Ti)(Si, Al)$_2O_6$), ilmenite, chromite ($FeCr_2O_4$), rutile and olivine ((Mg, Fe)$_2SiO_4$)[19,20] as the potential active components for CO_2 photothermal catalysis (PTC) for the proposed EP pathway. XRD, TEM and Brunauer-Emmett-Teller (BET, Extended Data Fig. 7) analyses also showed that the CE-5 sample is rich of porous zeolite-like structure, which might increase the reactive surface area for EP processes.

A series of solar-based catalytic technologies were applied with CE-5 lunar soil. The three-electrode configuration PV-EC technology was firstly investigated. The CE-5 lunar soil was used as both the anodic electrocatalyst (e-catalyst) for oxygen evolution reaction (OER), and the cathodic e-catalyst for hydrogen evolution reaction (HER). The overpotential @ 10 mA·cm^{-2} were 460 mV for OER, and 570 mV for HER, respectively (Figure S1, S2). While the two-electrode configuration electrolytic system was connected to a 5-series Si solar cells (area of 6.5 cm^2 per cell, 15% efficiency, Fig. 2a, S2b), the solar-to-hydrogen (STH) efficiency of 1% could be achieved with 1/15 PV electricity @ 2.90 V. Obvious H_2 and O_2 bubbles could be observed on the surface of electrodes (Fig. S2a, movie S1), which shows the possibility for the utilization of CE-5 lunar soil in the PV-EC technology. The relatively poor stability (Fig. S2c), could be caused by electrochemical corrosion of carbon substrate and lunar soil at the anode side. Further investigation is needed to improve PV-EC efficiency and stability. The PC full water splitting was also studied for comparison and resulted in unstable catalytic performance (Fig. S3) that was probably caused by the poor dispersity and light-driven self-corrosion.

The CE-5 lunar soil was also used as the photocatalyst to evaluate CO_2 reduction in aqueous condition with UV-vis irradiation. The sample exhibited CO rate of 6.07 ± 1.83 μmol· g^{-1}· h^{-1}, and the CH_4 yield of 0.20 ± 0.12 μmol· g^{-1}· h^{-1} without the presence of H_2, with a ~96.8% CO selectivity. The lunar sample was also studied as the photothermal catalyst towards CO_2 hydrogenation at the temperature close to moon environment (150ºC). Surprisingly, the products mainly consist of methanol and methane which can be considered as the foundation of organic synthesis and the fuel additive, respectively. The methanol and methane rate are ~22.2 and ~14.1 μmol· g^{-1}· h^{-1} with a methanol selectivity of ~62%. Excellent stability can also be observed within 10 cycles. Since it is barely to detect the methanol from the PT batch system, to confirm the reliability of methanol, the product is collected and confirmed by the proton nuclear magnetic resonance spectroscopy (H-NMR, Fig. S4). Isotopically labeled $^{13}CH_3OH$ was also tested via

high resolution mass spectroscopy (HRMS) to confirm that the methanol is originated from CO_2, but not adventitious carbon contamination (Fig. S5).

Based on the aforementioned catalytic performances of distinct solar-based technologies, a combined solar energy conversion pathway, namely extraterritorial photosynthesis, is proposed (Fig. 3). Although the current catalytic performance from the CE-5 lunar sample cannot satisfied the requirement of extraterrestrial survival, significant improvement could be achieved via structure optimization, morphological modification and composition engineering of the lunar sample. This work provides a potential strategy to build an *in-situ* resource utilization system that can accommodate to the extreme lunar temperature environment (Fig. S6), and only requires solar energy, water and lunar soil on the moon. Based on this system, we can realize a 'zero energy consumption' environment and life support system, and truly support lunar exploration, research and travelling.

References

1 https://blogs.nasa.gov/Watch_the_Skies/2009/06/15/post_1245073749119/.

2 https://solarsystem.nasa.gov/moons/earths-moon/in-depth/.

3 Logan, L. M. & Hunt, G. R. Infrared emission spectra: enhancement of diagnostic features by the lunar environment. *Science* **169**, 865-866 (1970).

4 Stubbs, T. J. *et al.* Dependence of lunar surface charging on solar wind plasma conditions and solar irradiation. *Planet Space Sci* **90**, 10-27 (2014).

5 Fears, F. D. Interplanetary bases-the moon and the orbital space station. *Journal of Space Flight* **3**, 4-5 (1951).

6 Christian Junaedi, K. H., Dennis Walsh, Subir Roychoudhury, Morgan B. Abney, Jay L. Perry. Compact and lightweight sabatier reactor for carbon dioxide reduction. *41st International Conference on Environmental Systems (ICES)*, 20120016419 (2011).

7 Chevallier, F., Feng, L. A., Bosch, H., Palmer, P. I. & Rayner, P. J. On the impact of transport model errors for the estimation of CO2 surface fluxes from GOSAT observations. *Geophys Res Lett* **37**, L21803 (2010).

8 Hecht, M. *et al.* Mars oxygen ISRU EXPeriment (MOXIE). *Space Sci Rev* **217**, 9 (2021).

9 Yang, L. Q. *et al.* Extraterrestrial artificial photosynthetic materials for in-situ resource utilization. *Natl Sci Rev* **8**, nwab104 (2021).

10 Hayne, P. O., Aharonson, O. & Schorghofer, N. Micro cold traps on the Moon. *Nat Astron* **5**, 169-175 (2021).

11 Anand, M. *et al.* A brief review of chemical and mineralogical resources on the Moon and likely initial in situ resource utilization (ISRU) applications. *Planet Space Sci* **74**, 42-48 (2012).

12 Sanders, G. B. & Larson, W. E. Progress made in lunar in situ resource utilization under NASA's exploration technology and development program. *J Aerospace Eng* **26**, 5-17 (2013).

13 https://odr.io/lunar-regolith-xrd#/search/display/713/eyJkdF9pZCI6IjQyNCJ9/1.

14 Fujishima, A. & Honda, K. Electrochemical photolysis of water at a semiconductor electrode. *Nature* **238**, 37-38 (1972).

15 Balan, A. P. *et al.* A non-van der waals two-dimensional material from natural titanium mineral ore ilmenite. *Chem Mater* **30**, 5923-5931 (2018).

16 Zhou, G. *et al.* Photoinduced semiconductor-metal transition in ultrathin troilite FeS nanosheets to trigger efficient hydrogen evolution. *Nat Commun* **10**, 399 (2019).

17 Sharma, S., Sivalingam, K., Neese, F. & Chan, G. K. L. Low-energy spectrum of iron-sulfur clusters directly from many-particle quantum mechanics. *Nat Chem* **6**, 927-933 (2014).

18 Hausmann, J. N. *et al.* Evolving highly active oxidic iron(III) phase from corrosion of intermetallic iron silicide to master efficient electrocatalytic water oxidation and selective oxygenation of 5-hydroxymethylfurfural. *Adv Mater* **33**, 2008823 (2021).

19 Cai, M. J. *et al.* Greenhouse-inspired supra-photothermal CO_2 catalysis. *Nat Energy* **6**, 807-814 (2021).

20 Ghoussoub, M., Xia, M. K., Duchesne, P. N., Segal, D. & Ozin, G. Principles of photothermal gas-phase heterogeneous CO_2 catalysis. *Energ Environ Sci* **12**, 1122-1142, doi:10.1039/c8ee02790k (2019).

21 Holder, C. F. & Schaak, R. E. Tutorial on powder X-ray diffraction for characterizing nanoscale materials. *ACS Nano* **13**, 7359-7365 (2019).

22 Scherrer, P., Bestimmung der inneren Struktur und der Größe von Kolloidteilchen mittels Röntgenstrahlen. In *Kolloidchemie Ein Lehrbuch*, Springer: p 387-409 (1912).

23 Downs, R. T. H.-W., M., The American Mineralogist Crystal Structure Database. American Mineralogist 88, 247-250 (2003).

24 Lee, J.-W.; Park, W. B.; Lee, J. H.; Singh, S. P.; Sohn, K.-S., A deep-learning technique for phase identification in multiphase inorganic compounds using synthetic XRD powder patterns. *Nat. Commun. 11*, 1-11 (2020).

25 Oviedo, F.; Ren, Z.; Sun, S.; Settens, C.; Liu, Z.; Hartono, N. T. P.; Ramasamy, S.; DeCost, B. L.; Tian, S. I.; Romano, G., Fast and interpretable classification of small X-ray diffraction datasets using data augmentation and deep neural networks. *NPJ Comput. Mater. 5*, 1-9 (2019).

26 Maas, A. L.; Hannun, A. Y.; Ng, A. Y. In *Rectifier nonlinearities improve neural network acoustic models*, Proc. icml, Citeseer: p3 (2013).

Declarations

Acknowledgement

We are thankful to all the staff of China's Chang'E Lunar Exploration Project for their hard work in returning lunar samples. The samples studied in this work were allocated by the China National Space Administration (Sample No. CE5C0400). This work was supported primarily by the National Key Research and Development Program of China (2020YFA0710302), the Major Research Plan of the National Natural Science Foundation of China (91963206), the National Natural Science Foundation of China (52072169, 51627810, 51972164, 51972167), the Fundamental Research Funds for the Central Universities (14380193), the Program for Guangdong Introducing Innovative and Enterpreneurial Teams (2019ZT08L101), the Natural Science Foundation of Jiangsu Province (SBK2018022120), the open fund of Wuhan National Laboratory for Optoelectronics (2018WNLOKF020), the Fundamental Research Funds for the Central Universities (14380193), Civil Aerospace Technology Research Project(B0108): Extraterrestrial In-situ water Extraction and photochemical synthesis of hydrogen and oxygen, and Foshan Xianhu Laboratory of the Advanced Energy Science and Technology Guangdong Laboratory.

Methods

Material characterizations

The morphology of samples were investigated using a Zeiss ultra-plus thermal field-emission scanning electron microscopy (FESEM, Carl Zeiss SMT AG, Germany) and transmission electron microscopy (TEM, Tecnai G2 F20). The crystal structure of the films was obtained by X-ray diffraction (Ultima III, Rigaku Corp.). The surface composition of the samples was characterized by using X-ray photoelectron spectroscopy (XPS, ESCALAB 250) with the non-monochromatic Al K_{α} X-ray as the X-ray source. The BET surface was measured through Brunauer-Emmett-Teller (BET) method (TriStar-3000, Micromeritics, USA).

XRD Machine Learning

Data preparation

The XRD spectra are known to exhibit different behaviors according to the sample size, orientation, and morphology[21]. The Scherrer equation[22] relates the size of sub-micrometer crystallites in a solid to the

broadening of a peak in a diffraction pattern. The preferred orientation by stacking one facet eliminates the XRD signals of facets from other families. The morphologies can lead to different max interplanar distance and cause some larger-distance facet signal to disappear.

Raw data were downloaded from the American Mineralogist Crystal Structure Database[23]. As the database contains too many kinds of minerals, and the real XRD data of their mixture is not enough, the data was first augmented to construct a database. First, no more than twenty minerals were selected as the components and their proportions assigned randomly. As the element analysis has limited the element composition to no more than O, Si, Al, Fe, Ca, Mg, P, S, Cr, structures containing elements beyond these were ignored. Second, a random morphology with size and orientation was assigned for each of them. According to the Scherrer equation and the size, some peaks were broadened and some vanished, which led to the XRD for each component. Finally, the XRD signal were summed with weights equal to the proportions.

Algorithms (experimental section)

The existence of the minerals was trained and calculated using a 1D convolutional neural network (CNN) as a binary classification model[24,25]. We here provided a CNN based algorithm to examine the XRD spectra for the sample compositions and proportions. Consecutive convolution layers with number of channels 8, 8, 16, 16, 32, 32, 64, 64 with kernel size 5 and stride 1 were connected with a max pooling layer every two convolutional layers. LeakyReLUs[26] were added after the convolutions layers for nonlinearity. Such a binary classification model was present for each of the mineral possible.

After obtaining the most probable components, the total XRD signal was fitted using the components' XRD signals via a least square fitting. During the fitting, the facet families were used separately as independent basis since the XRD is anisotropic, i.e. peaks of (001) and (002) are dependent. However either of them is independent from (111). The intensity ratio of the peak families could vary due to the 3D shape of the crystallite. The XRD basis were no longer rigid ones from the bulk materials, but a soft basis by flexible 3D crystallites. For example, one peak could be larger than the others due to orderly stacking of the facet, or that the crystallite was larger along its lattice vector. This explains the abnormally high peaks in the high-theta range, where some specific peaks of the components are prominent.

The size of the grain crystallite domain could be approximate by Scherrer equation

$$D = \frac{Kv}{B\cos\theta}$$

where D is the mean size of the ordered crystalline domains which may be smaller or equal to the grain size and particle size, K the dimensionless shape factor close to 1, v the X-ray wavelength, B the full width of the peak at half maximum (FWHM), and θ the Bragg angle. It requires the overview upon the whole

facet family for the complete information. Also, the size solved from the same facet family is expected to be the same.

Photovoltaic-electrocatalytic measurement

Preparation of the OER and HER electrode

The CE-5 lunar soil ink was prepared by dissolving 10 mg CE-5 lunar soil into 400 μL ethanol and 50 μL Nafion (5 wt%) and sonicated for 20min. Then, 100 μL ink was dropped onto 1 cm × 1 cm Carbon paper and dried in the air. Next, the CE-5 lunar soil coated CP and cellulose membrane were tightly connected to electrode clips.

Electrochemical measurements

The electrochemical characterization was carried out with a CHI 760e electrochemical workstation. The photothermal promoted water splitting performance was measured in 1M KOH solution. The working electrode was raised above the liquid level and the cellulose membrane attached to the back side of working electrode supplied electrolyte for it. Besides, the reference electrode, counter electrode and electrolytic tank were all wrapped by aluminum foil, so the light irradiation and temperature rise had no influence on the calibration of the measured potential. All the measured potential values were calibrated following the equation of:

$$E_{RHE} = E_{Hg/HgO} + 0.095 + 0.592 * pH$$

Where E_{RHE} and $E_{Hg/HgO}$ is reversible hydrogen electrode potential and Hg/HgO electrode potential, respectively. PH is the pH value of electrolyte. The indoor temperature and humidity was ~25 ºC and 50% respectively if not mentioned otherwise.

Photocatalytic measurement

Measurement of photocatalytic activity:

For the photocatalytic reduction of CO_2, 23 mg of CE-5 lunar soil was uniformly dispersed on the glass reactor with an area of 4.2 cm^2. A 300 W Xenon arc lamp was used as the light source of the photocatalytic reaction. The volume of the reaction system was about 460 ml. Before the irradiation, the system was vacuum-treated several times, and then the high purity of CO_2 gas was pumped into the

reaction setup for reaching ambient pressure. 0.4 mL of deionized water was injected into the reaction system as a reducer. The CE-5 lunar soil were allowed to equilibrate in the CO_2/H_2O atmosphere for several hours to ensure that the adsorption of gas molecules was complete. During the irradiation, about 1 mL of gas was continually taken from the reaction cell at given time intervals for subsequent CO, CH_4, and H_2 concentration analysis by using a gas chromatograph (GC-2014C, Shimadzu Corp., Japan).

Photocatalytic full water splitting experiments were performed in a gas-tight system fitted with a side window of optical flat quartz glass. 20 mg of CE-5 lunar soil was used as catalysts dissolved into 50 ml of pure water. Then the suspension was stirred in a sealed glass vessel during which lunar soil was not good dispersive, and purged with Ar for 30 min prior to photocatalytic experiments to remove dissolved oxygen. A 300 W Xenon arc lamp was used as the light source of the photocatalytic reaction. During the photocatalytic reaction, the reactor was placed in a thermoregulated rack at room temperature with magnetic stirring to ensure a constant temperature and uniform irradiation. The amount of evolved H_2 and O_2 gas was measured simultaneously using an online gas chromatography system (GC-8A, Shimadzu Corp., Japan) with a thermal conductivity detector (TCD) and Ar as the carrier gas.

Photothermal catalytic measurement

The photothermal measurement is conducted under 0.4 MPa mixture gas with an H2:CO2 ratio of 4:1. The catalyst (~3-5 mg) was drop casted onto a silica fiber holder, dried out overnight, and tested in a photothermal batch reactor (WGHX-50, Xi'an Taikang Biological Technology Co., Ltd.) with external heat of 150 ºC. The 300W Xe lamp (PLS-SXE300BF, Beijing Perfectlight Technology Co., Ltd.) provides irradiation with a light intensity of roughly 17 suns. Each test cycle needed 1 hour and the products were tested by Gas chromatography (Panna A91Plus, Changzhou Panna Instrument Co., Ltd.). The product was also purged into D_2O for liquid proton NMR (Bruker Avance NEO 500, Bruker Corporation) as well. Isotopically labeled tracing experiments were performed with $^{13}CO_2$ (99.9 at%, Energy Chemical). Isotope distributions in the product gases were measured using HRMS (Waters Xevo G2-XS QT, Waters Corporation).

Figures

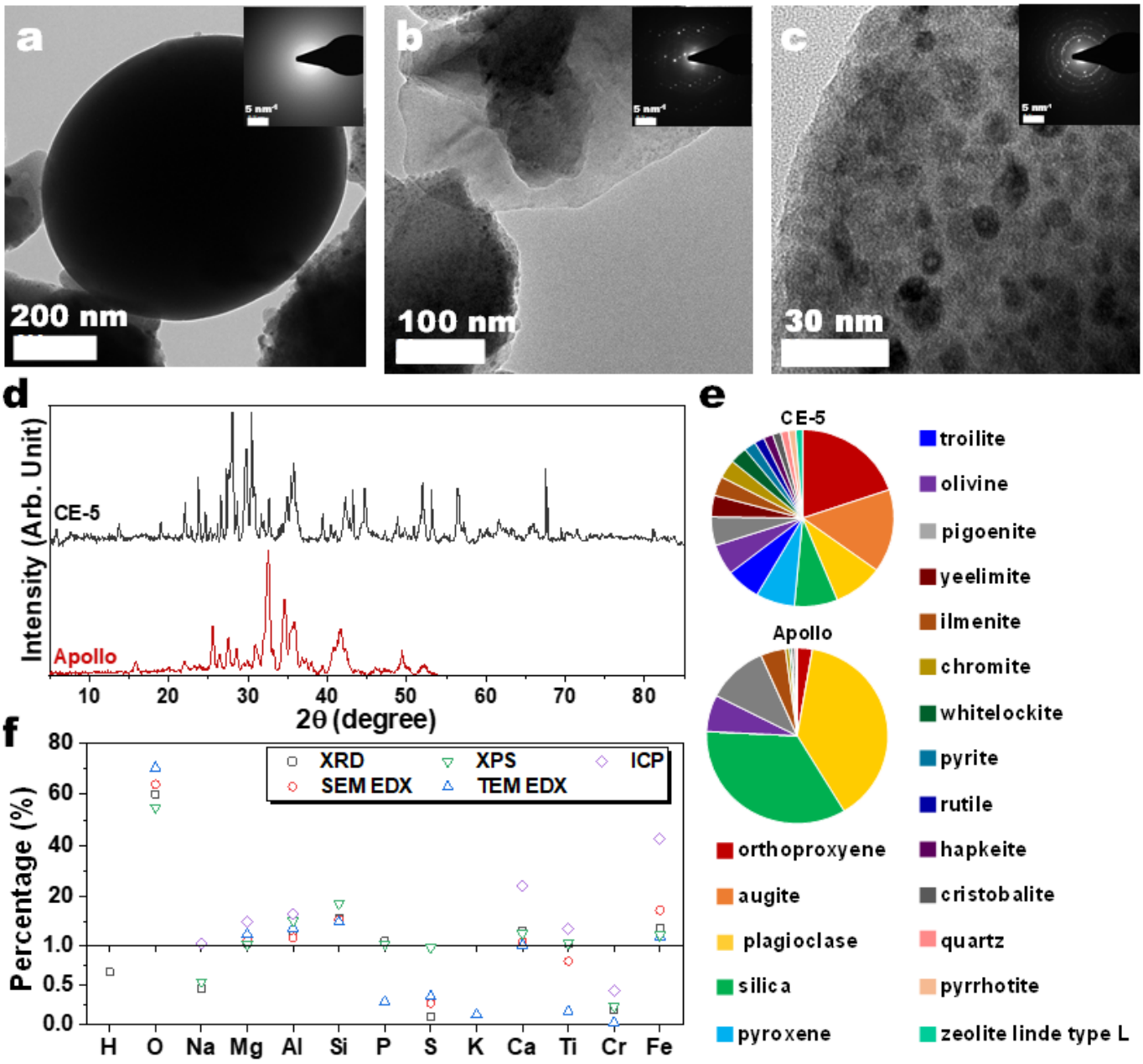

Figure 1

Material Characterization of CE-5 samples with comparison to Apollo-12 sample (No. 12041)13. Transmission electron microscopy (TEM) images CE-5 lunar soil sample with a) glassy phase, b) single-crystalline sheet, and c) porous structure. Inset of a-c): electron diffraction patterns . d) X-ray diffraction (XRD) patterns of the CE-5 lunar soil sample and the Apollo data. e) Material composition based on the CE-5 sample and the Apollo data analyzed by XRD machine learning. And f) Element components of the CE-5 sample analyzed by XRD, X-ray photoelectron spectra (XPS), scanning electron microscopy (SEM) energy dispersive X-Ray spectroscopy (EDX), transmission electron microscopy (TEM) EDX, and inductive coupled plasma emission spectrometer (ICP), respectively. The percentage of metal elements detected by ICP was relatviely higher, since nonmetallic elements, such as O, Si, S, P, could not be detected through ICP.

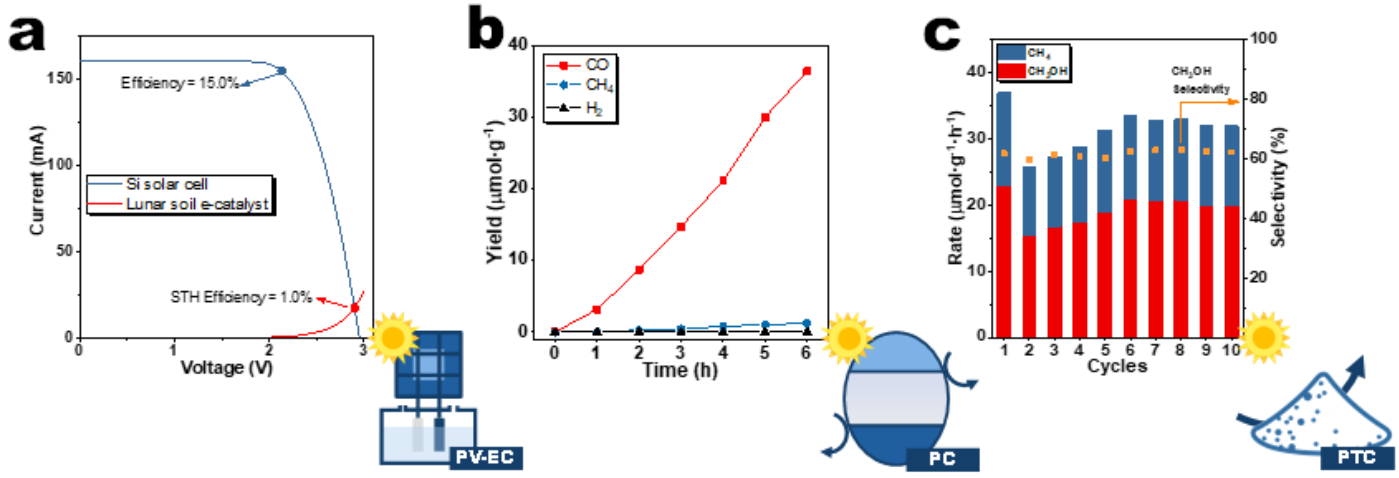

Figure 2

Catalytic performance of lunar soil. a) PV-EC process for water splitting. The CE-5 lunar soil was used as both the hydrogen evolution reaction (HER), and the oxygen evolution reaction (OER) electrocatalysts (e-catalysts). b) PC process for CO2 reduction. The lunar soil was used as the CO2 reduction photocatalyst. c) PTC process for CO2 hydrogenation. The lunar soil was used as the PT catalyst.

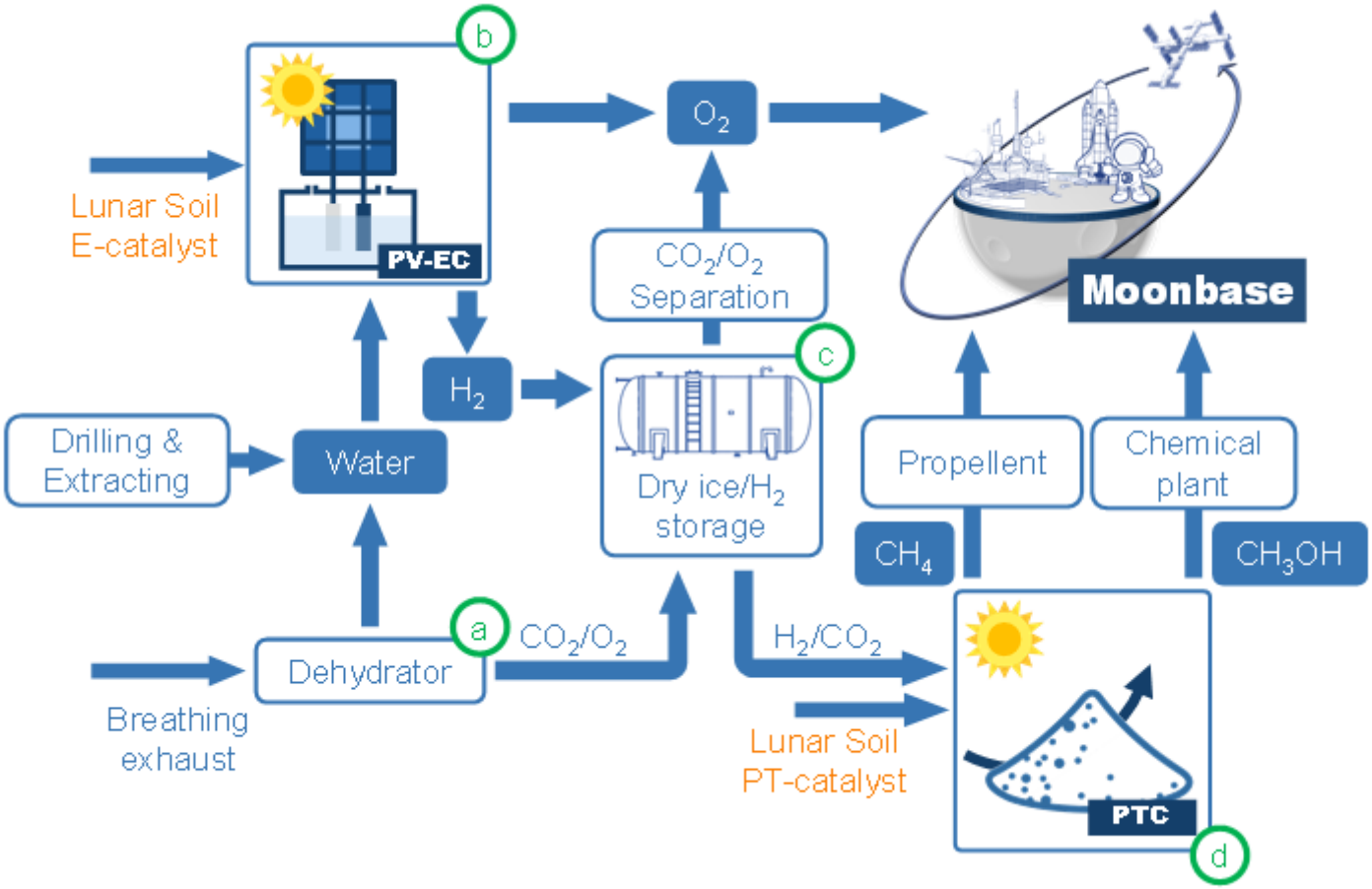

Figure 3

Proposed EP strategy. a) Breathing exhaust (containing H_2O, CO_2, and O_2) passes through the dehydrator to separate H_2O and form dry CO_2 and O_2. The separated H_2O is added to drilled and extracted water for drinking and PV-EC process.10 The CO_2 and O_2 gas is transferred to the gas vessel. b) With the solar irradiation, PV-EC is performed for H_2 and O_2 generation with the lunar soil e-catalyst, whereas H_2 is transferred to the gas vessel, and O_2 is used for breathing. c) Since the temperature at night is as low as -173°C, CO_2 congeals into dry ice with proper pressure maintained by H_2. d) At daytime, the moon temperature rise to around 127°C, suitable for PTC CO_2 hydrogenation with the lunar soil. Among the resulting PT product, CH_4 can be used as the fuel and propellant, and CH_3OH can be used as the building block for essential chemicals. All of the mentioned products could eventually improve the feasibility and durability of human survival on the moon.

Supplementary Files

This is a list of supplementary files associated with this preprint. Click to download.

- ExtendedData.docx
- SupplementaryInformation.docx
- MovieS1.mp4